A simple TOPMODEL-based runoff parameterization (SIMTOP) for use in global climate models

Guo-Yue Niu and Zong-Liang Yang

Department of Geological Sciences, John A. and Katherine G. Jackson School of Geosciences, University of Texas, Austin, Texas, USA

Robert E. Dickinson

School of Earth and Atmospheric Sciences, Georgia Institute of Technology, Atlanta, Georgia, USA

Lindsey E. Gulden

Department of Geological Sciences, John A. and Katherine G. Jackson School of Geosciences, University of Texas, Austin, Texas, USA

Received 21 April 2005; revised 25 July 2005; accepted 18 August 2005; published 8 November 2005.

[1] This paper develops a simple TOPMODEL-based runoff parameterization (hereinafter SIMTOP) for use in global climate models (GCMs) that improves the runoff production and the partitioning of runoff between surface and subsurface components. SIMTOP simplifies the TOPMODEL runoff formulations in two ways: (1) SIMTOP represents the discrete distribution of the topographic index as an exponential function, not as a three-parameter gamma distribution; this change improves the parameterization of the fractional saturated area, especially in mountainous regions. (2) SIMTOP treats subsurface runoff as a product of an exponential function of the water table depth and a single coefficient, not as a product of several parameters that depend on topography and soil properties; this change facilitates applying TOPMODEL-based runoff schemes on global scale. SIMTOP is incorporated into the National Center for Atmospheric Research (NCAR) Community Land Model version 2.0 (CLM 2.0). SIMTOP is validated at a watershed scale using data from the Sleepers River watershed in Vermont, USA. It is also validated on a global scale using the monthly runoff data from the University of New Hampshire Global Runoff Data Center (UNH-GRDC). SIMTOP performs favorably when compared to the baseline runoff formulation used in CLM2.0. Realistic simulations can be obtained using two distinct saturated hydraulic conductivity (K_{sat}) profiles. These profiles include (1) exponential decay of K_{sat} with depth (as is typically done in TOPMODEL-based runoff schemes) and (2) the definition of K_{sat} using the soil texture profile data (as is typically done in climate models) and the concordant reduction of the gravitational drainage from the bottom of the soil column.

Citation: Niu, G.-Y., Z.-L. Yang, R. E. Dickinson, and L. E. Gulden (2005), A simple TOPMODEL-based runoff parameterization (SIMTOP) for use in global climate models, *J. Geophys. Res.*, *110*, D21106, doi:10.1029/2005JD006111.

1. Introduction

[2] Runoff is one of the major components of the global water cycle and accounts for about 40% of the precipitation on land. As such, it plays an important role in the global climate system by affecting evapotranspiration and freshwater inputs to the oceans, which in turn affects the ocean thermohaline circulation. A model's runoff formulation helps control its soil moisture, which influences the latent heat flux between the land surface and the atmosphere. However, its inclusion in climate models has been problematic.

[3] Runoff is conceptually difficult to represent in climate models. The environmental factors that control runoff, precipitation, soil moisture, and topography, often vary considerably on local scales. Furthermore, data that can be used to validate runoff production are difficult to obtain. Streamflow data provide a proxy measurement for runoff integrated across watersheds; streamflow observations provide statistical constraints on the development of conceptual-statistical runoff models. The paucity of such statistical constraints and the plethora of conceptualizations for runoff schemes have led to a wide variety of implementations. Recent land model intercomparison projects [*Bowling et al.*, 2003; *Boone et al.*, 2004] summarized various implementations of runoff schemes ranging from simple bucket models to more sophisticated topography-based runoff models. The partitioning of precipitation

0148-0227/05/2005JD006111$09.00

into evapotranspiration, surface runoff and subsurface runoff (baseflow) varies widely among these land models. Climate models have been adjusted so that the global, multiyear average runoff production is about 1/3 of the average precipitation. Runoff is divided approximately equally between surface and subsurface runoff to match the early observational estimates [*Dickinson et al.*, 1993].

[4] Hydrologists introduced the concept of fractional saturated area as the dominant control on surface runoff. In such schemes, precipitation that falls over the saturated fraction of a model grid cell is immediately converted to surface runoff. The fractional saturated area is conceptually correlated with near-surface soil moisture as it is represented in the BATS model [*Dickinson et al.*, 1993]. More recent implementations [*Famiglietti and Wood*, 1994; *Stieglitz et al.*, 1997; *Koster et al.*, 2000; *Ducharne et al.*, 2000; *Chen and Kumar*, 2001; *Yang and Niu*, 2003; *Niu and Yang*, 2003; *Gedney and Cox*, 2003] define the fractional saturated area as a function of the topography and the water table depth (or water deficit depth) following TOPMODEL [*Beven and Kirkby*, 1979; *Sivapalan et al.*, 1987]. *Warrach et al.* [2002] showed that TOPMODEL may be superior to the Variable Infiltration Capacity (VIC) model [*Liang et al.*, 1994], because the former explicitly represents topographic effects on the subgrid soil moisture distribution and has fewer calibration parameters. TOPMODEL incorporates topographic variation using the concept of "topographic index" or "wetness index," $\lambda = \ln(a/\tan\beta)$, where a is the specific catchment area, i.e., the upstream area above a pixel that drains through the unit contour at the pixel and $\tan\beta$ is the local surface topographic slope. *Famiglietti and Wood* [1994] proposed a discretized framework in which the distribution of the topographic index was disaggregated into a number of bands, each representing a fraction of the watershed with similar water table depth and soil moisture, to parameterize the subgrid variability in soil moisture and runoff. However, its structural conflicts with climate models and its high computation costs impeded its application to climate models. More recent applications [*Stieglitz et al.*, 1997; *Ducharne et al.*, 2000; *Chen and Kumar*, 2001; *Niu and Yang*, 2003] used a three-parameter gamma distribution function to represent the discrete distribution of the topographic index. This approach is more computationally efficient than the discretized framework and is structurally consistent with climate models, but it is likely to be inaccurate in mountainous regions because of the failure of the three-parameter gamma distribution to fit the discrete distribution of the topographic index in areas with steep, variable slopes.

[5] Climate models and TOPMODEL use dramatically different definitions of the soil saturated hydraulic conductivity, K_{sat}. Climate models usually define K_{sat} as a function of soil texture, while TOPMODEL assumes that K_{sat} decreases with soil depth to create a water table. In TOPMODEL, the soil surface value of K_{sat} is an arbitrary parameter because it is solely used to produce runoff. However, a climate model uses the soil hydraulic properties to determine soil moisture, which in turn affects evaporation and transpiration. The original derivations of the TOPMODEL subsurface runoff [*Sivapalan et al.*, 1987] require much larger values for the soil surface K_{sat} than do climate models; researchers justified the very large K_{sat} with arguments about the role of macropores [e.g., *Beven*, 1982]. For instance, *Stieglitz et al.* [1997] increased the soil surface K_{sat} used in climate models by a factor of 1,000 in their application of a TOPMODEL-based runoff scheme to a Soil-Vegetation-Atmosphere Transfer (SVAT) scheme. Consequently, the soil hydraulic properties in their SVAT are dramatically distorted from those usually used in climate models.

[6] Although the assumptions of the very high surface K_{sat} and the decay of K_{sat} with soil depth are crude approximations of reality [*Beven*, 1997], TOPMODEL's use of topographic index to explicitly use topographic data to describe the subgrid soil moisture variability captures the critical differences between upslope and downslope hydrological behavior [*Koster et al.*, 2000].

[7] This study develops a simple TOPMODEL-based runoff parameterization (SIMTOP) that mitigates several of the problems with TOPMODEL-based runoff schemes for use in climate models. SIMTOP uses a maximum subsurface runoff coefficient in place of a complex product of coefficients. This simplification makes the parameterized subsurface runoff independent of the soil surface K_{sat} defined by the soil texture profile. To parameterize the surface saturated area, SIMTOP also represents the discrete distribution of the topographic index with an exponential function instead of a three-parameter gamma distribution function. In such a way, SIMTOP accommodates the topographic data using a single topographic parameter, the potential or maximum fractional saturated area, $F_{\max}$. $F_{\max}$ is defined as the ratio of the number of pixels whose topographic indexes are equal to or larger than the grid cell mean topographic index to the total number of pixels in a grid cell or a catchment.

[8] This study is different from those of *Famiglietti and Wood* [1994], *Stieglitz et al.* [1997], *Ducharne et al.* [2000], and *Chen and Kumar* [2001], which used the hydrological catchment as the fundamental land unit. This study applies the TOPMODEL concept to rectangular grid cells which can avoid the uncertainties caused by downscaling atmospheric forcing variables from a GCM grid cell to its contained catchments and upscaling surface fluxes from the catchments to a GCM grid cell. Although a large, rectangular GCM grid cell may encompass many small catchments, the statistics of the topographic index still have hydrological meaning because pixels with similar topographic index values are assumed to behave in a hydrologically similar manner [*Quinn et al.*, 1995].

[9] Precipitation is arguably the dominant control on the spatial variability of runoff on short timescales. Thus basins of a scale comparable to or smaller than the spatial extent of rainfall during individual precipitation events are most suitable for testing the performance of runoff schemes on short timescales. The performance of SIMTOP in predicting runoff is first evaluated at a small spatial and temporal scale using daily runoff data observed in a subcatchment of the Sleepers River watershed [*Stieglitz et al.*, 1997]. Then SIMTOP is evaluated on a global, monthly scale with the monthly runoff data of the University of New Hampshire – Global Runoff Data Center (UNH-GRDC) [*Fekete et al.*,

2000]. The model is evaluated by employing "model efficiency," *ME* [see also *Warrach et al.*, 2002]:

$$ME = \frac{\left[\sum_{i=1}^{N}(O_i - \overline{O})^2 - \sum_{i=1}^{N}(S_i - O_i)^2\right]}{\left[\sum_{i=1}^{N}(O_i - \overline{O})^2\right]} \quad (1)$$

where N is the total length of data; O_i and S_i denote the observed and simulated value at day i, and $\overline{O}$ is the observed mean value. *ME* is a measure of the model ability to simulate the observed runoff amplitudes, which are dominated by surface runoff. The higher *ME* is, the better a model performs. *Boone et al.* [2004] reported models that produced larger ratios of surface runoff to the total runoff generally resulted in lower model efficiency.

2. Model

[10] We use the National Center for Atmospheric Research (NCAR) Community Land Model version 2.0 (CLM2.0) [*Bonan et al.*, 2002] in this study. The Community (also "Common") Land Model [*Dai et al.*, 2003] is a point land model that is used as the land component of the Community Climate System Model (CCSM). The model's hydrology of the more recent CLM 3.0 [e.g., *Oleson et al.*, 2004] is identical to that of CLM 2.0; differences between CLM 2.0 and CLM 3.0 are not believed to have any noticeable impact on the simulations reported here.

[11] Because of the lack of generally robust procedures to obtain subgrid precipitation intensities from the grid cell mean forcing provided by the atmospheric model, CLM 2.0 produces an excess of canopy interception loss [*Bonan et al.*, 2002]. When assessing the performance of runoff schemes, the fraction of precipitation reaching the soil surface needs to be as accurate as possible. A simple scheme for calculating subgrid precipitation is used in this study to reduce the excessive interception of precipitation by the canopy and thus to allow more water to reach the soil surface. The fractional area of precipitation can be estimated as:

$$f_p = \frac{P_l + P_c}{P_l + 10 \times P_c} \quad (2)$$

where f_p is the fraction of the grid cell on which precipitation falls, P_l is the large-scale precipitation and P_c is the convective precipitation. When there is purely convective precipitation f_p = 0.1 and when there is no convective precipitation f_p = 1.0. In the default CLM, the intercepted fraction of precipitation by the canopy is $f_i = 1 - e^{-LSAI}$, where *LSAI* is the leaf and stem area index of the canopy. In this study, f_p is used to modify f_i: $f_i = fd(1 - e^{-LSAI})$. Consequently, the canopy-intercepted fraction of precipitation is reduced by a factor of f_p. Note that equation (2) changes only the amount of precipitation intercepted by the canopy not the precipitation rate. Because our goal is to address TOPMODEL-related issues, we omit discussion of how the location of the fractional precipitation over saturated or unsaturated areas affects runoff production.

[12] In the following subsections, we describe the baseline runoff scheme in CLM, the TOPMODEL-based scheme of *Chen and Kumar* [2001] and SIMTOP. SIMTOP is proposed as a replacement for the baseline runoff scheme in CLM.

2.1. Baseline Runoff Scheme in CLM

[13] CLM 2.0 has 10 soil layers and a soil profile depth of 3.43 m. The baseline runoff scheme in CLM is a hybrid of the runoff schemes of BATS [*Dickinson et al.*, 1993] and TOPMODEL. Following TOPMODEL, the saturated hydraulic conductivity decreases exponentially with soil depth:

$$K_{sat}(z) = K_{sat}(0)e^{-fz} \quad (3)$$

where $K_{sat}(0)$ is the soil surface value of K_{sat}, which is based on *Cosby et al.* [1984]. The decay factor, f, can be determined through sensitivity analysis or calibration against the hydrograph recession curve. In the default CLM 2.0, f is set to 2.0.

[14] The baseline runoff scheme partitions runoff, R, into surface runoff, R_s, and subsurface runoff, R_{sb}. Surface runoff is the sum of runoff from saturated and unsaturated fractional areas:

$$R_s = F_{sat}Q_{wat} + (1 - F_{sat})w_s^4 Q_{wat} \quad (4)$$

where Q_{wat} is the input of water (sum of rainfall, dewfall, and snowmelt) incident on the soil surface and w_s is the layer depth–weighted wetness over the first three layers, which have a combined depth of 0.091 m. The first term is also used by TOPMODEL to describe surface runoff. Part of the second term ($w_s^4 Q_{wat}$) is the BATS surface runoff scheme, which was introduced into CLM to parameterize the infiltration excess surface runoff over unsaturated areas. The fractional saturated area is:

$$F_{sat} = F_{\max}e^{-D} \quad (5)$$

where D is a dimensionless water deficit depth (see *Oleson et al.* [2004] for detail). $F_{\max}$ is set to 0.3 in the default CLM 2.0.

[15] Total subsurface runoff is

$$R_{sb} = F_{sat}l_b e^{-D} + (1 - F_{sat})K_{sat}(z_b)w_{bm}^{2B+3} + \sum_{i=1}^{10}\max[0, ((\theta_i - \theta_e)\Delta z_i/\Delta t)] \quad (6)$$

The first term is similar to the subsurface runoff formulation in TOPMODEL for the saturated area; l_b is the maximum subsurface runoff coefficient when the entire soil column is saturated. The second term follows BATS and represents the gravitational drainage from the bottom of the soil column, where $K_{sat}(z_b)$ is the saturated hydraulic conductivity at the model bottom, which is the maximum bottom drainage rate when the bottom soil is saturated. w_{bm} is the hydraulic-conductivity-weighted average of the wetness in the bottom three layers. $K_{sat}(z_b)$ is 0.04 mm s^{-1} (as calibrated against the Red-Arkansas watershed streamflow data), a value that

exceeds any likely precipitation rates. B is a parameter that depends on soil texture [*Clapp and Hornberger*, 1978]. The third term is the "oversaturated" water, which results from solving soil moisture using a tridiagonal matrix. The volumetric soil moisture of the ith layer is θ_i and θ_e is the soil effective porosity (the residual of porosity minus ice volume). Δz_i and Δt are the soil layer depth of the ith layer and the timestep, respectively.

2.2. TOPMODEL-Based Runoff Scheme

[16] In the TOMODEL-based runoff scheme of *Chen and Kumar* [2001], the surface macropores are represented by enhancing the surface saturated hydraulic conductivity, $K_{sat}(0)$, as follows [see also *Wolock*, 1993]:

$$K_{sat}(0) = K_{sat} e^{fd_c} \tag{7}$$

where d_c is the depth over which macropores influence soil hydraulic conductivity and the value of the "compacted" K_{sat} is defined by the soil texture according to *Cosby et al.* [1984]. *Chen and Kumar* [2001] assumed that d_c = 1.0 m. This representation is consistent with the concept of soil surface macropores [*Beven*, 1982].

[17] Surface runoff consists of overland flow by the Dunne mechanism, which generates surface runoff when rain falls on saturated ground, and overland flow by the Horton mechanism, which generates overland flow when the rainfall rate exceeds the infiltration capacity of the soil. The mathematical representation of the above processes takes the form of:

$$R_s = F_{sat} Q_{wat} + (1 - F_{sat}) \max(0, (Q_{wat} - I_{\max})) \tag{8}$$

where $I_{\max}$ is the soil infiltration capacity dependent on soil texture and moisture conditions [*Entekhabi and Eagleson*, 1989]. *Stieglitz et al.* [1997] and *Niu and Yang* [2003] demonstrated that the second term is negligible for TOPMODEL-based approaches, especially when the surface macropore assumption is applied. The saturated fraction of the soil is determined by the topographic characteristics and soil moisture state of a grid cell:

$$F_{sat} = \int_{\lambda \geq (\lambda_m + f z_\nabla)} pdf(\lambda) d\lambda \tag{9}$$

where $\lambda = \ln(a/\tan\beta)$ is the topographic index at a pixel, where a is the specific catchment area and $\tan\beta$ is the local surface topographic slope [*Quinn et al.*, 1995; *Wolock and McCabe*, 1995]. λ_m is the grid cell mean value of λ; $pdf(\lambda)$ is the probability density function of λ. z_∇ is the grid cell mean water table depth.

[18] Following *Sivapalan et al.* [1987], the subsurface runoff is expressed as:

$$R_{sb} = \frac{\alpha K_{sat}(0)}{f} e^{-\lambda_m} e^{-f z_\nabla} \tag{10}$$

where α is the anisotropic factor, the importance of which is further justified by *Kumar* [2004]. In TOPMODEL, the "oversaturated" water in a subsurface soil layer is added to the overlying soil layer instead of being added to subsurface runoff as in the baseline CLM runoff scheme.

[19] To calculate soil moisture, a bottom boundary condition is required. It is assumed that the hydraulic conductivity at the bottom, $K(z_b)$, is given as: $K(z_b) = K_{sat}(z_b) w_b^{2B+3}$, where z_b is the bottom depth of the soil column, $K_{sat}(z_b)$ is the saturated hydraulic conductivity at the model bottom, and w_b is the soil wetness of the bottom layer. Because it is uncertain that the model bottom with a depth of 3.43 m reaches the impermeable bedrock, water flow from the bottom soil layer is treated as an additional source of subsurface runoff. Because K_{sat} decays exponentially with depth, $K_{sat}(z_b)$ is very small when the decay factor f is large, and thus the bottom drainage is negligible compared to total subsurface runoff. If $K_{sat}(z_b)$ is assumed to depend on the soil texture at the bottom, $K(z_b)$ may be of comparable magnitude to R_{sb}. The effects of $K(z_b)$ on runoff simulations will be discussed later.

2.3. SIMTOP Runoff Scheme

[20] In SIMTOP, equations (9) and (10) are simplified. The saturated fraction is parameterized as

$$F_{sat} = F_{\max} e^{-C_s f z_\nabla} \tag{11}$$

where C_s is a coefficient that can be derived by fitting the exponential function to the discrete cumulative distribution function (CDF) of the topographic index. $F_{\max}$, the maximum saturated fraction for a grid cell, is defined as the CDF of the topographic index when the grid cell mean water table depth is zero. Therefore $F_{\max}$ is the percent of pixels in a grid cell or a catchment whose topographic indexes are larger than or equal to the grid cell mean topographic index, λ_m. $F_{\max}$ is estimated to be 0.42 for the Sleepers River watershed (Figure 1). The calculation of $F_{\max}$ for global continents will be discussed later. As shown in Figure 1a, the exponential function $F_{\max} e^{-C_s(\lambda - \lambda_m)}$ (C_s = 0.5) agrees very well with the three-parameter gamma distribution function when the topographic index is larger than or equal to the catchment mean topographic index, λ_m. The CDF of the topographic index can be converted to the fractional saturated area as a function of the water table depth when the topographic index ($\lambda - \lambda_m$) is scaled by f (Figure 1b). The agreement of $F_{\max} e^{-C_s f z_\nabla}$ (C_s = 0.5) with the CDF of the three-parameter gamma distribution as shown in Figure 1b demonstrates that equation (11) has the same behavior as equation (9) in determining the fractional saturated area. However, without C_s (or C_s = 1.0), the $F_{\max} e^{-f z_\nabla}$ curve, used by *Niu and Yang* [2003], underestimates the fractional saturated area and hence surface runoff.

[21] In SIMTOP, subsurface runoff is parameterized as:

$$R_{sb} = R_{sb,\max} e^{-f z_\nabla} \tag{12}$$

where $R_{sb,\max}$ is the maximum subsurface runoff when the grid cell mean water table depth is zero. Equation (12) is similar to the subsurface runoff formulation in the original TOPMODEL [*Beven and Kirkby*, 1979]. In SIMTOP, $R_{sb,\max}$ is a single calibration parameter instead of a product of α, $K_{sat}(0)$, $1/f$, and $e^{-\lambda_m}$. This simplification avoids the

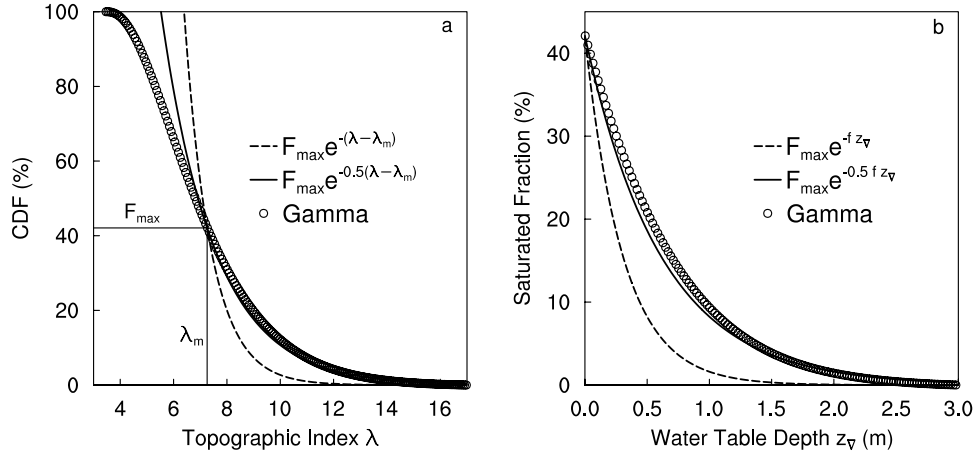

Figure 1. (a) Cumulative distribution function (CDF) of the analytical three-parameter gamma function (circles) as a function of topographic index in comparison with the fitted curves of $F_{\max}e^{-0.5(\lambda-\lambda_m)}$ (solid line) and $F_{\max}e^{-(\lambda-\lambda_m)}$ (dashed line) and (b) fractional saturated area as a function of the grid mean water table depth plotted with the fitted curves of $F_{\max}e^{-0.5\ fz_\nabla}$ (solid line) and $F_{\max}e^{-fz_\nabla}$ (dashed line).

difficulties in determining the surface saturated hydraulic conductivity in the lateral direction ($\alpha K_{sat}(0)$) and the uncertainties that result from computing the mean topographic index (λ_m) with coarse-resolution Digital Elevation Model (DEM) data (1 km × 1 km) currently available for all continents.

2.4. Water Table Depth

[22] Following *Chen and Kumar* [2001], SIMTOP and the TOPMODEL-based runoff scheme solve the water table depth by assuming that the water head at depth z is in equilibrium with that at the water table (z_∇):

$$\psi(z) - z = \psi_{sat} - z_\nabla \tag{13}$$

where $\psi(z)$ and ψ_{sat} are the matric potential at depth z and the matric potential at saturation, respectively. z_∇ is the water table depth. Substituting $\psi(z)$ in equation (13) with the one of *Clapp and Hornberger* [1978], we get:

$$\psi_{sat}\left(\frac{\theta(z)}{\theta_{sat}}\right)^{-B} - z = \psi_{sat} - z_\nabla \tag{14}$$

where $\theta(z)$ is the volumetric water content at depth z and θ_{sat} is the volumetric water content at saturation. The resulting soil moisture profile is:

$$\theta(z) = \theta_{sat}\left(\frac{\psi_{sat} - (z_\nabla - z)}{\psi_{sat}}\right)^{-1/b} \tag{15}$$

The water table depth, z_∇, is then computed by solving the following equation iteratively:

$$D_\theta = \int_0^{z_\nabla} (\theta_{sat} - \theta(z))dz \tag{16}$$

where D_θ is the soil moisture deficit for the entire column. D_θ is calculated from the soil moisture profile, $D_\theta = \sum_{i=1}^{10}(\theta_{sat} - \theta_{liq,i})\Delta z_i$, where $\theta_{liq,i}$ is the volumetric liquid water content at the ith layer.

[23] One should bear in mind that two major assumptions are made to derive the water table depth: (1) The depth of the soil column is limited to only a few meters (3.43 m in CLM) and (2) the water head throughout the column is at equilibrium. These assumptions restrict the applicability of the above approach to regions where the water table is relatively shallower and times when the water table is in approximate equilibrium with the soil moisture in model soil layers. When the water table is deeper than the model bottom, the water table is decoupled from the soil moisture but may still contribute to baseflow. For such a case, a simple lumped aquifer model is suggested for use in GCMs.

2.5. Subsurface Runoff Removing Scheme

[24] In SIMTOP and the TOPMODEL-based scheme, the subsurface runoff is extracted from the soil liquid water mass in each soil layer in proportion to the hydraulic conductivity k_i of each layer weighted by the layer depth, Δz_i:

$$R_{sb}(i) = R_{sb}\left(k_i\Delta z_i / \sum_{i=1}^{10} k_i\Delta z_i\right) \tag{17}$$

3. Basin-Scale Model Evaluation

3.1. Data

[25] To evaluate the performance of each of the runoff schemes at a basin scale, we used observational data obtained in subcatchment W-3 (8.4 km^2) of the Sleepers River watershed (111 km^2), located in the highlands of Vermont, USA. The data set provides meteorological and hydrological data obtained between 1969 and 1974 at 1-hour intervals. The W-3 topography is characterized by rolling hills, and the soils are dominated by silty loams. The local vegetation is approximately one third grassland, one third

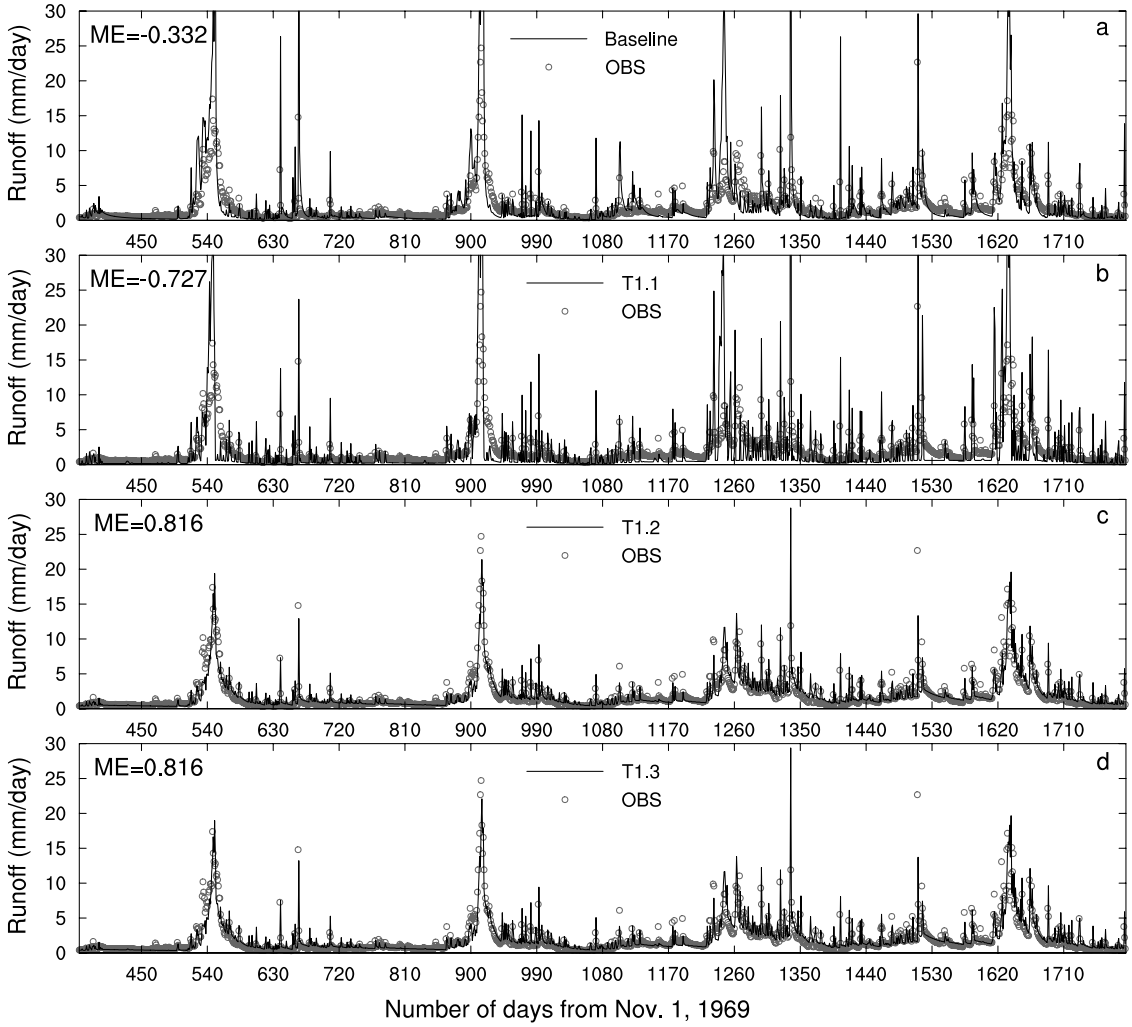

Figure 2. Model-predicted runoff from (a) the baseline runoff model, (b) TOPMODEL (T1.1 in Table 1), (c) TOPMODEL (T1.2 in Table 1), and (d) TOPMODEL (T1.3 in Table 1).

coniferous forest, and one third deciduous forest. Additional details about the Sleepers River watershed data set are provided by *Stieglitz et al.* [1997] and *Warrach et al.* [2002].

3.2. Experiments and Results

[26] We used the Sleepers River watershed data set to force CLM 2.0 with the baseline runoff formulation, and the output from this run was used as a control for comparison with later runs using SIMTOP and the TOPMODEL-based runoff scheme. The model was integrated for 5 years from November 1969 to November 1974. To limit the uncertainties introduced by the unknown initial soil moisture, we analyzed the last 4 years' data. As shown in Figure 2a, the baseline runoff scheme (without calibration to the model parameters) in CLM 2.0 overestimates the runoff peaks and underestimates runoff in recession periods. During snowmelt and rainfall events, the baseline scheme in CLM 2.0 produces an excessive amount of surface runoff mainly because of the redundant representations of surface runoff in equation (4). Correspondingly, the modeling efficiency of the baseline runoff scheme is -0.332. The very low modeling efficiency of the baseline model mainly results from the high ratio of surface runoff to the total runoff (0.490, as listed in Table 2).

[27] We conducted experiments to address the following questions: (1) Can TOPMODEL-based runoff formulations be configured so that they maintain reasonable runoff production when K_{sat} is kept vertically constant, as it usually is in climate models? (2) How well does SIMTOP perform when compared to the baseline CLM runoff formulation and TOPMODEL? (3) How do individual model calibration parameters affect the model's performance in simulating runoff and the soil moisture profile?

[28] To address question 1 above, we performed two sets of runs (see Table 1). In the first set of runs, we used the Sleeper's River watershed data to drive CLM 2.0 equipped with the TOPMODEL-based runoff scheme (equations (9) and (10)). In all three runs, K_{sat} decays exponentially with depth. In each of the three runs, we varied the components of the maximum subsurface runoff coefficient, $\frac{\alpha K_{sat}(0)}{f} e^{-\lambda_m}$, in equation (10). The modeled runoff production from the three runs is shown in Figures 2b–2d. Run T1.1 (Figure 2b), in which $K_{sat}(0)$ is derived from the soil properties of the Sleepers River watershed data set (1.3×10^{-3} mm s^{-1}) and

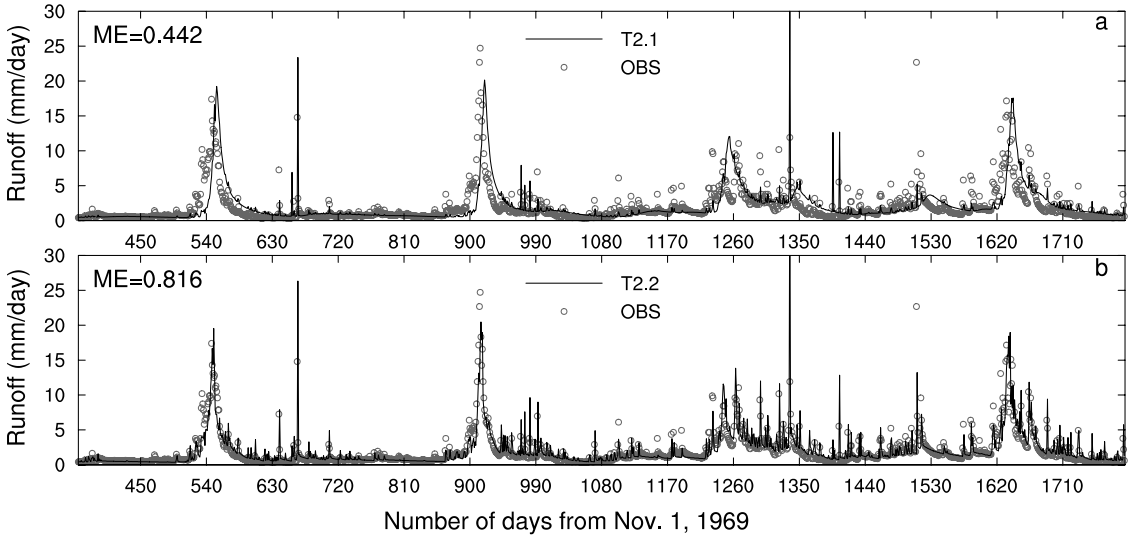

Figure 3. Model-predicted runoff compared to the observed. (a) TOPMODEL (T2.1 in Table 1) and (b) TOPMODEL (T2.2 in Table 1).

in which $K_{sat}(0)$ is scaled only by e^{fd_c} ($e^{fd_c} = e^{3.26\times1} = 26.05$), fails to predict the observed runoff. The model efficiency of T1.1 is very low (−0.727).

[29] The model parameters of T1.2 are identical to those of T1.1, except the subsurface runoff formulation is also scaled by the anisotropic factor, which is optimized in this study to a value of 19.69. T1.2, which is equivalent to the version of *Chen and Kumar* [2001], succeeds in capturing both the peaks and recession curves and has a much higher model efficiency (0.816) (Figure 2c) than T1.1 (Figure 2b) and the baseline CLM runoff model (Figure 2a). The third run excludes the anisotropic factor but uses an optimized $K_{sat}(0)$ value of 0.66 mm s^{-1} (508 times larger than 1.3×10^{-3} mm s^{-1}). This third case, equivalent to the version of *Stieglitz et al.* [1997], also succeeds in reproducing observed runoff (Figure 2d). T1.2 and T1.3 both increase the subsurface runoff coefficient by a factor of about 500; however, the soil-column integrated $K_{sat}(0)$ value used in T1.2 is of an order of magnitude comparable to that typically used in climate models because the anisotropic factor, not $K_{sat}(0)$, increases the subsurface runoff coefficient.

[30] Accurate determination of the anisotropic factor is difficult, especially for global applications. This first set of experiments shows that the simplified subsurface runoff formulation of SIMTOP (equation (12)), in which a single calibration parameter $R_{sb,\max}$ replaces the complex product of calibration parameters $\left(\frac{\alpha K_{sat}(0)}{f} e^{-\lambda_m}\right)$, can be applied with negligible effect on model efficiency. Using the optimized parameters obtained in the first set of runs (α = 19.69, $K_{sat}(0) = 1.31 \times 10^{-3} \times e^{3.26}$, λ_m = 7.26, and f = 3.26), we estimated the optimized value of $R_{sb,\max}$ for the Sleepers River watershed to be 1.448×10^{-4} mm s^{-1}.

[31] In the second set of experiments using the TOPMODEL-based runoff scheme, we analyzed how runoff production responds to a vertically constant K_{sat} when bottom drainage is allowed (T2.1) and when bottom drainage is not allowed (T2.2). For both runs, surface runoff is calculated using equation (9), subsurface runoff is calculated using equation (12) ($R_{sb,\max} = 1.448 \times 10^{-4}$ mm s^{-1}), and K_{sat} is derived from soil texture data and kept vertically constant at a value of 1.3×10^{-3} mm s^{-1}. In T2.1, the bottom drainage ($K_{sat}(z_b)w_b^{2B+3}$), not the TOPMODEL subsurface runoff function ($R_{sb,\max}e^{-fz_\nabla}$), dominates subsurface runoff. Because transport of soil water from the surface to the bottom of the soil column takes more time than does the subsurface runoff by the water table, the modeled runoff from T2.1 occurs later than the observed (Figure 3a). In T2.2, the simulated water table rises because no water drains from the bottom. T2.2 performs much better than T2.1 in simulating the timing of the runoff. We conclude from this pair of runs that, with the aid of the simplified subsurface runoff formulation (equation (12)), a vertically constant K_{sat} used in conjunction with a no−bottom drainage boundary condition can be used in place of the exponentially decaying K_{sat} without sacrificing model efficiency.

[32] To compare the performance of SIMTOP and the TOPMODEL-based runoff scheme, we conducted a series of four runs, the results of which are summarized in Table 2. In all four experiments, subsurface runoff was calculated

Table 1. Parameters Used in Simulations With TOPMODEL-Based Runoff Schemes

Version Code	K_{sat} Profile	Bottom Drainage	Subsurface Runoff Formulation	$R_{sb,\max}$, mm s^{-1}	$K_{sat}(0)$, mm s^{-1}	α
T1.1	exponential decay	yes	equation (10)	···	$1.3 \times 10^{-3} \times e^{3.26}$	1.0
T1.2	exponential decay	yes	equation (10)	···	$1.3 \times 10^{-3} \times e^{3.26}$	19.96
T1.3	exponential decay	yes	equation (10)	···	0.66	1.0
T2.1	constant	yes	equation (12)	1.448×10^{-4}	1.3×10^{-3}	···
T2.2	constant	no	equation (12)	1.448×10^{-4}	1.3×10^{-3}	···

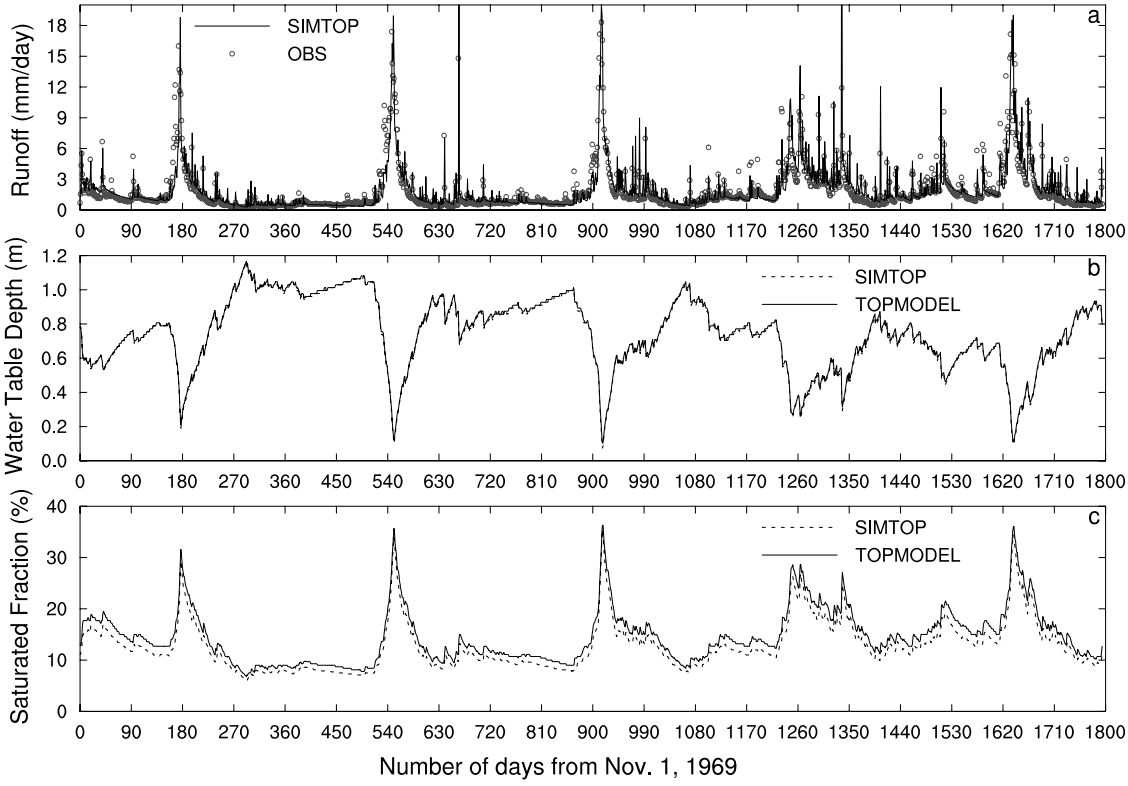

Figure 4. Modeled (a) runoff with SIMTOP (S2 in Table 2), (b) water table depth, and (c) fractional saturated area with SIMTOP and TOPMODEL (T2 in Table 2).

using equation (12). The TOPMODEL-based runoff scheme calculated the saturated fraction using equation (9); SIMTOP calculated the saturated fraction using equation (11).

[33] We ran two pairs of experiments. Each pair had one run, in which K_{sat} decays exponentially with depth but is enhanced by surface macropores, and one run, in which K_{sat} is kept vertically constant and the bottom is sealed The TOPMODEL-based scheme was used in one pair of runs (version codes T1 and T2 in Table 2) and SIMTOP in the other pair (S1 and S2 in Table 2). SIMTOP and the TOPMODEL-based scheme performs equally well in producing runoff for various saturated hydraulic conductivity profiles. The values of the optimum parameters for all simulations (T1, T2, S1, and S2) were nearly the same. Figure 4a shows that SIMTOP (S2) does a decent job in reproducing the observed discharge. The simulated water table depth and fractional saturated area by SIMTOP and the TOPMODEL-based scheme are essentially the same in magnitude and variability (Figures 4b and 4c).

[34] We analyzed the sensitivity of the model (T2 and S2 in Table 2) to two calibration parameters, the decay factor (f) and the maximum subsurface runoff coefficient ($R_{sb,\max}$). A value of f between 3.0 and 4.0 m^{-1} and a value of $R_{sb,\max}$ between 1.0×10^{-4} to 3.0×10^{-4} mm s^{-1} produced the highest model efficiencies (Figures 5c and 6c).

[35] The volume of total runoff is not sensitive to different values of f and $R_{sb,\max}$ (Figures 5a and 6a) because the long-term accumulated runoff in both the TOPMODEL and SIMTOP frameworks is predominantly controlled by precipitation and the energy available for evapotranspiration. When compared to baseline runoff model, the TOPMODEL-based simulations and the SIMTOP simulations produce significantly less total runoff (Table 2), indicating that runoff schemes are more important than the value of runoff parameters in controlling the total runoff volume. However, the values of both f and $R_{sb,\max}$ significantly affect the partitioning of runoff into the fast-response surface component and the slow-response subsurface com-

Table 2. Results From Runs Comparing the Baseline CLM 2.0 Runoff Scheme, the TOPMODEL-Based Runoff Scheme, and the SIMTOP Runoff Scheme[a]

Schemes	Baseline CTRL	TOPMODEL		SIMTOP	
		T1	T2	S1	S2
K_{sat} profiles	E	EM	CB	EM	CB
Optimum f	2.0	3.26	3.28	3.26	3.26
Optimum $R_{sb,\max}$ ($\times 10^{-4}$)	0.1	1.45	1.484	1.36	1.46
Model efficiency	−0.332	0.816	0.817	0.817	0.827
RMSE	0.087	0.032	0.032	0.032	0.031
CR	0.836	0.903	0.906	0.904	0.910
Total runoff	2.447	2.121	2.129	2.121	2.123
R_{st}	0.490	0.301	0.311	0.276	0.280
sm1	0.547	0.690	0.705	0.695	0.707
sm2	0.484	0.727	0.739	0.734	0.741
sm3	0.586	0.907	0.900	0.713	0.902

[a]RMSE stands for root mean square error; CR for correlation coefficient; R_{st} for the ratio of surface runoff to the total runoff; and sm1, sm2 and sm3 stand for the soil saturation rate within the soil profile segments ranging from 0.0–0.1 m, 0.1–1.0 m, and 1.0–3.43 m, respectively; K_{sat} profile, E stands for exponential decay of K_{sat}; EM for exponential decay of K_{sat} with surface macropores; CB for the vertically constant K_{sat} without bottom drainage.

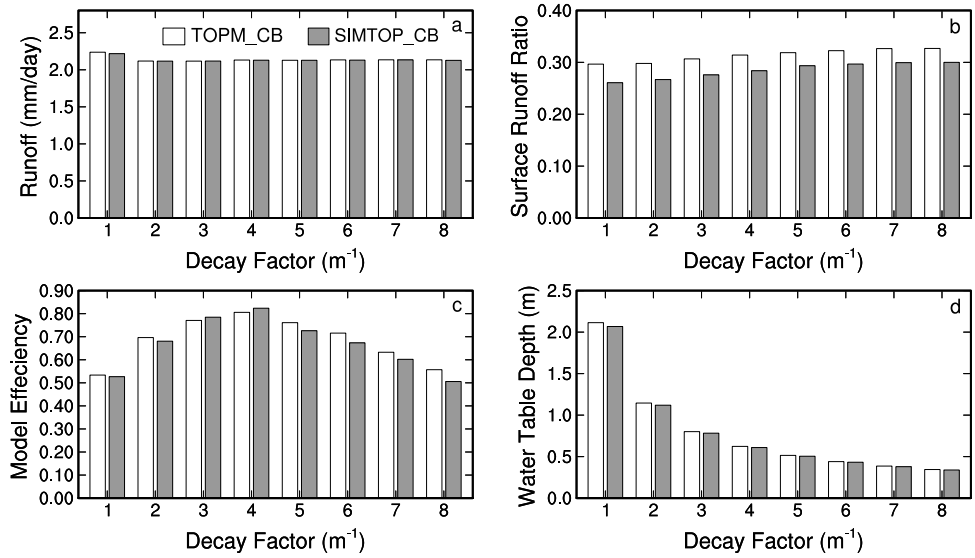

Figure 5. Modeled 4-year-averaged (a) total runoff, (b) ratio of surface runoff to the total runoff, (c) model efficiency, and (d) water table depth varied with the decay factor, *f*, of the TOPMODEL (open bar in Figure 5 and T2 in Table 2) and SIMTOP (shaded bar in Figure 5 and S2 in Table 2).

ponent (Figures 5b and 6b). It is well known that the decay factor, *f*, controls the shape and timing of the hydrograph recession curve and hence the seasonality of runoff and evapotranspiration.

[36] The water table depth is affected by variations in both *f* and $R_{sb,\max}$. Increasing *f* decreases the water table depth (Figure 5d); increasing $R_{sb,\max}$ increases the water table depth (Figure 6d). *f* can also affect the seasonality of the water table depth. The soil moisture profiles are also very sensitive to the value of *f* and $R_{sb,\max}$ (Figures 7a and 7b). Larger *f* results in wetter soil, while larger $R_{sb,\max}$ results in drier soil. The above sensitivity analyses indicate that *f* and $R_{sb,\max}$ control the total volume and seasonality of the watershed water storage by affecting the magnitude of surface runoff.

4. Estimation of $F_{\max}$, the Potential or Maximum Fractional Saturated Area

[37] The topographic index data used in this study are downloaded from the HYDRO1K Elevation Derivative Database in the Land Processes Distributed Active Archive Center (LPDAAC), a part of NASA's Earth Observing System (EOS) Data and Information System (EOSDIS)

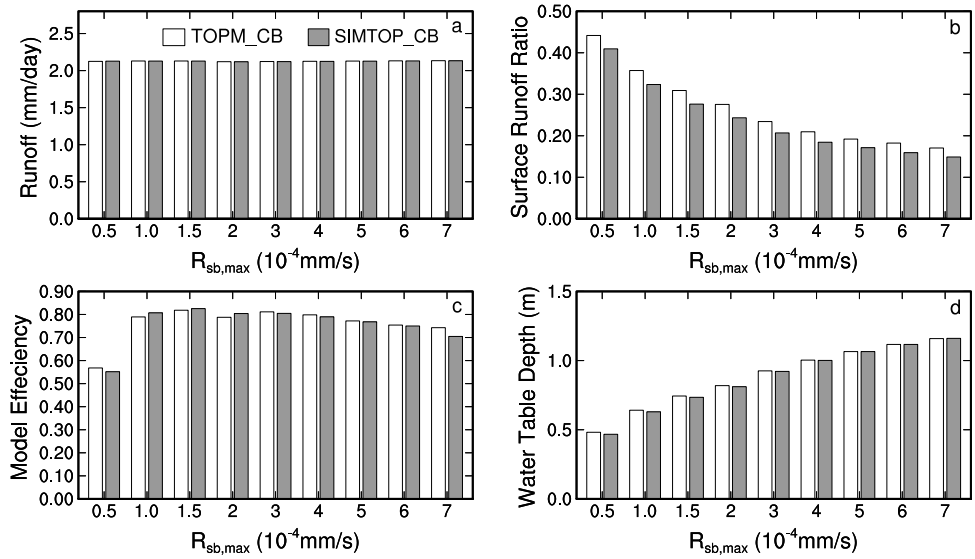

Figure 6. Modeled 4-year-averaged (a) total runoff, (b) surface runoff ratio to the total runoff, (c) model efficiency, and (d) water table depth to the maximum subsurface runoff coefficient, $R_{sb,\max}$ of the TOPMODEL (open bar in Figure 6 and T2 in Table 2) and SIMTOP (shaded bar in Figure 6 and S2 in Table 2).

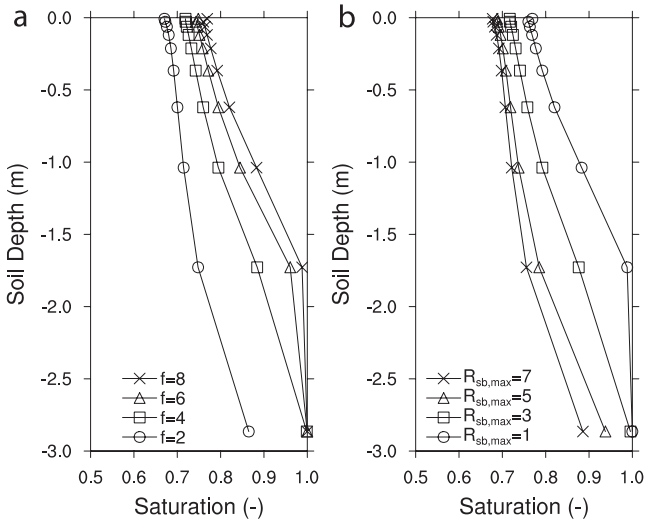

Figure 7. Sensitivity of soil moisture profile to (a) the decay parameter f and (b) the maximum subsurface runoff coefficient $R_{sb,\max}$ (10^{-4} mm s^{-1}), in the case of SIMTOP (S2 in Table 2).

initiative (see website: http://edcdaac.usgs.gov/gtopo30/hydro/index.asp). We first adjust the HYDRO1K topographic index calculated at 1000-m resolution to 100-m resolution using a regression equation proposed by *Wolock and McCabe* [2000] as follows:

$$\lambda_{100m} = 0.961 \times \lambda_{1000m} - 1.957 \tag{18}$$

The adjusted topographic index values are then used to derive the CDF. The CDF of a $1^\circ \times 1^\circ$ grid cell is derived by accumulating the PDF of the grid cell, which has about 10,000 1-km pixels in a midlatitude grid cell with each pixel having an adjusted topographic index. The CDF of the discrete distribution of the topographic index can be separated into two parts: the part where topographic index values are greater than or equal to the grid cell mean topographic index, λ_m and the part where topographic index are less than λ_m (Figure 8). The segment of the distribution with values at or above the mean represents the hydrological characteristics of the topography in lowland areas, while the segment with values below the mean represents those in the upland areas. In practice, it is not necessary to accurately capture the distribution where the topographic indices are less than λ_m (i.e., in upland areas) because, according to the TOPMODEL concept, the fractional saturated area is determined by the area where the topographic index, $\lambda \geq$

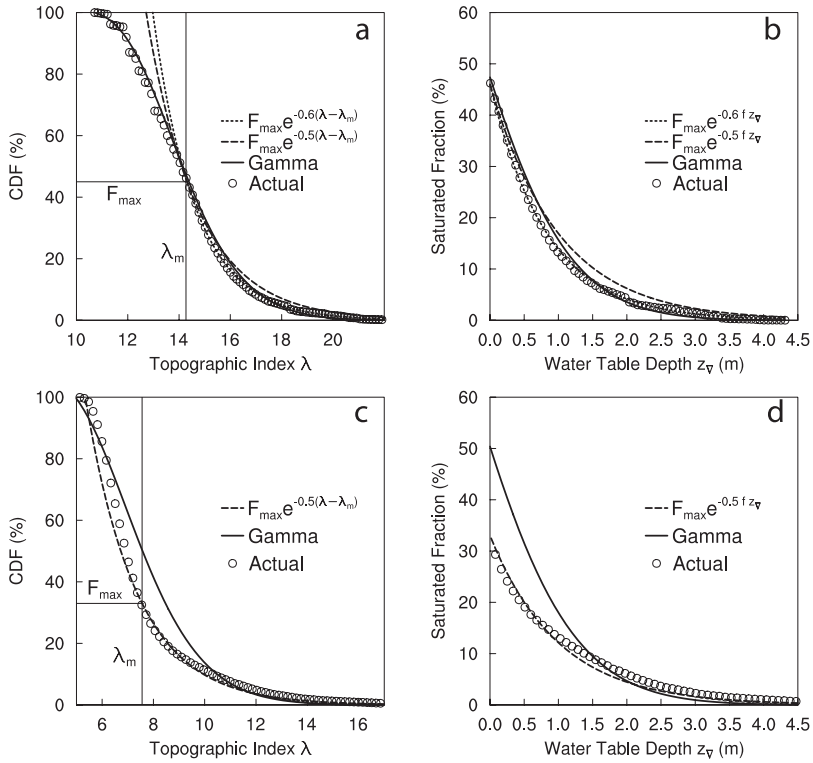

Figure 8. (a) Cumulative distribution function (CDF) (circles) computed from the discrete distribution of the topographic index in comparison with the fitted curves of the analytical three-parameter gamma distribution (solid line), $F_{\max}e^{-0.5(\lambda-\lambda_m)}$ (long dashed line), and $F_{\max}e^{-0.6(\lambda-\lambda_m)}$ (short dashed line). (b) Fractional saturated area varied with the grid mean water table depth in comparison with the fitted curves of the analytical three-parameter gamma distribution (solid line), $F_{\max}e^{-0.5\ fz_\nabla}$ (long dashed line), and $F_{\max}e^{-0.6\ fz_\nabla}$ (short dashed line) in a $1^\circ \times 1^\circ$ grid cell of the Amazon River basin. Note that the water table depth (x axis) $z_\nabla = (\lambda - \lambda_m)/f$. (c and d) Same as Figures 8a and 8b, respectively, but in a grid cell representing a segment of the northern Rocky Mountains.

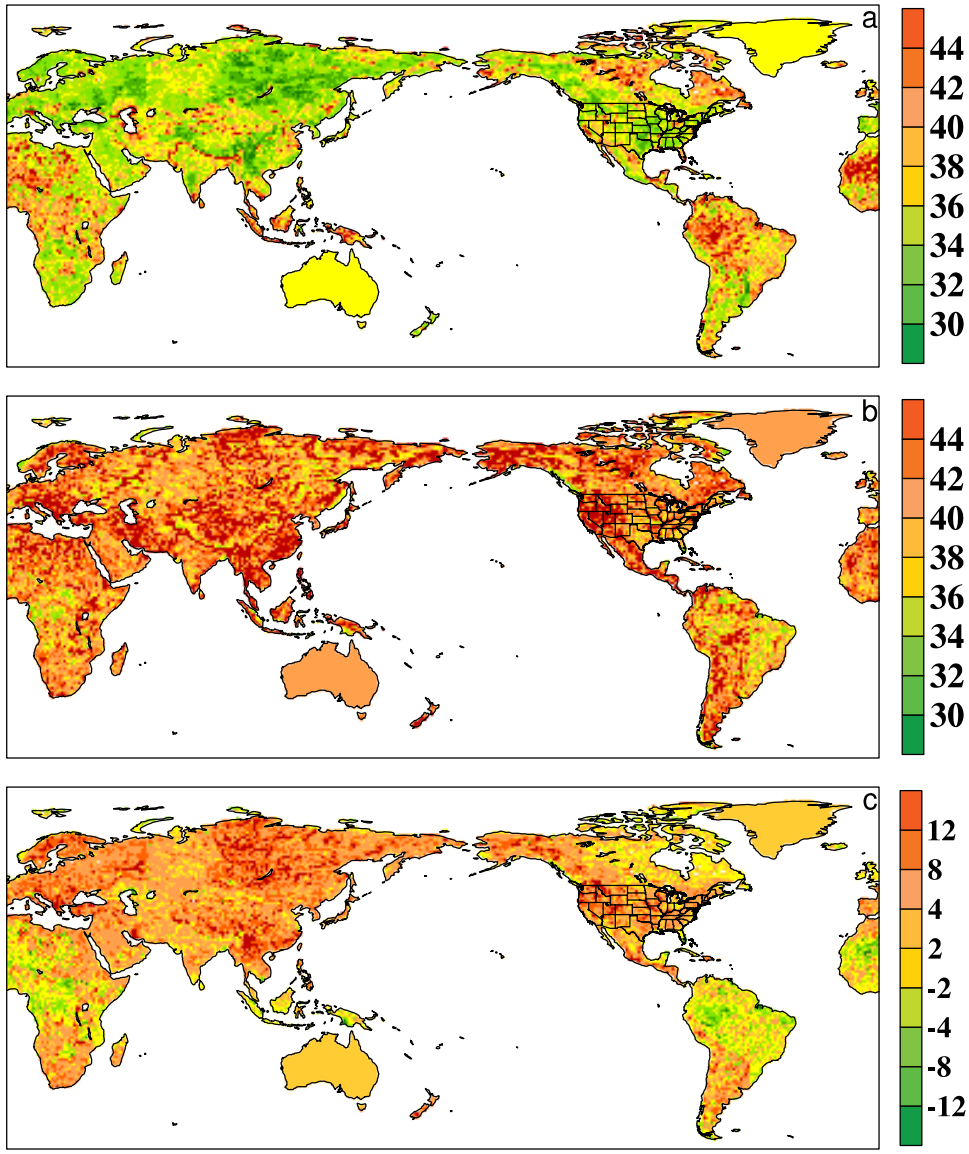

Figure 9. (a) Maximum saturated fractional area (%) at 1° × 1° determined with the discrete cumulative distribution function, (b) maximum saturated fractional area (%) at 1° × 1° determined with the cumulative distribution function of the three-parameter gamma function, and (c) Figure 9b minus Figure 9a.

$\lambda_m + fz_\nabla$. Therefore, we use an exponential function to fit the discrete distribution where $\lambda \geq \lambda_m$ (i.e., in lowland areas). The maximum fractional saturated area, F_{max}, is defined as the cumulative distribution function (CDF) of the topographic index when the grid cell mean water table depth is zero, i.e., $\lambda = \lambda_m$. The exponential function of $\lambda - \lambda_m$ scaled by F_{max} fits the discrete CDF very well in flat areas (Figure 8a) and in mountainous areas (Figure 8c). When the topographic index is converted to the water table depth by using the relationship $z_\nabla = (\lambda - \lambda_m)/f$, where $f = 2\ m^{-1}$, the variation of the fractional saturated area with the water table depth is obtained as shown in Figures 8b and 8d.

[38] The analytical three-parameter gamma distribution overestimates F_{max} by about 18 percent in a grid cell in the northern Rocky Mountains (Figure 8d); however, it agrees well with the discrete distribution in flat areas such as the Amazon River basin (Figure 8c). We computed both the discrete CDF and the three-parameter gamma distribution for each 1° × 1° grid-cell to estimate F_{max}. The three-parameter gamma distribution overestimates F_{max} by 8 to 12 percent in most mountainous regions and slightly underestimates F_{max} in flat regions such as the Amazon basin and the Congo River basin (Figure 9c) when compared to that determined from the discrete CDF (Figure 9a). As shown in Figure 9a, a greater value of F_{max} corresponds to more lowland pixels, while a lower value corresponds to more upland pixels in a grid cell. However, F_{max} derived from the analytical three-parameter gamma distribution (Figure 9b) fails to capture the global distribution of F_{max} computed from the discrete CDF. Because the two-parameter (F_{max} and C_s) exponential function is used to fit only the part of the discrete CDF where the topographic index is larger than its grid cell mean value, it performs better than the three-parameter analytical gamma function does. Moreover, it

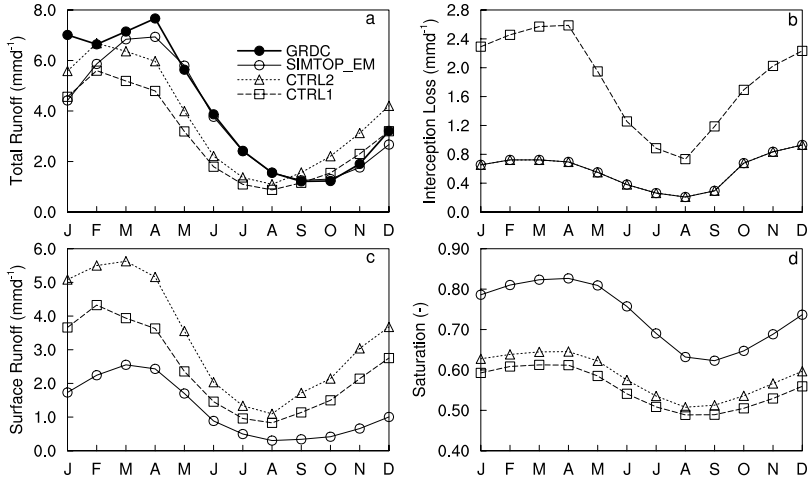

Figure 10. Model predicted (a) total runoff, (b) interception loss, (c) surface runoff, and (d) entire soil-column soil moisture from experiments CTRL1, CTRL2, and SIMTOP-EM for the Amazon Basin (0°–10°S, 50°–70°W). The UNH-GRDC runoff is also included in Figure 10a.

implies that the distribution of the topographic index in low land areas, where the terrain is more affected by the hydrological processes (e.g., erosion and sediment) than that in upland areas, follows an exponential law.

[39] The coefficient C_s = 0.5 performs very well in fitting the discrete CDF in the mountainous areas (Figures 8c and 8d), while C_s = 0.6 does better in flat areas (Figures 8a and 8b). However, because of the uncertainties involved in determining the water table depth, the decay factor (f), and the coarse resolution of DEM, a more elaborate determination of C_s is not expected to further improve the precision of the calculation of the fractional saturated area. Therefore, for the global-scale testing of SIMTOP, we use a globally constant value (C_s = 0.5), which is the same as for the Sleepers River watershed. Because the HYDRO1K data are not available for Australia or Greenland, we used the global mean value of $F_{\max}$ for these two regions.

5. Global-Scale Model Evaluation

5.1. Data

[40] To drive the CLM 2.0 simulations at a global scale, we used the Global Soil Wetness Project 2 (GSWP2) 1° × 1° 3-hourly, near-surface meteorological data for the years 1986–1995. The GSWP2 is a combination of the National Centers for Environmental Prediction (NCEP) and DOE model reanalysis data sets and the gridded observational data sets that were used in the International Satellite Land Surface Climatology Project Initiative II. The near-surface meteorological data set includes large-scale and convective precipitation, air temperature, air pressure, specific humidity, shortwave and longwave radiation, and wind speed. Precipitation data from the NCEP/DOE model reanalysis were hybridized with the Global Precipitation Climatology Centre and the Global Precipitation Climatology Project gauge data and then corrected using a catch ratio correction factor [*Zhao and Dirmeyer*, 2003] for the wind-caused gauge undercatch. However, the hybridized precipitation is excessively overcorrected in most cold regions in wintertime.

[41] To evaluate the performance of SIMTOP and the baseline CLM2 runoff formulation at a global scale, we used the University of New Hampshire – Global Runoff Data Center (UNH-GRDC) monthly climatological composite runoff data set, which combines observed river discharge with output from a water balance model that is driven by observed meteorological data. This data set preserves the accuracy of the observed discharge measurements and maintains the spatial and temporal distribution of simulated runoff, thereby providing the best available estimate of global terrestrial runoff [*Fekete et al.*, 2000].

5.2. Experiments and Results

[42] We sought to evaluate the performance of SIMTOP in simulating runoff on a global domain. Using the GSWP2 near-surface meteorological data, we conducted four experiments:

[43] 1. Experiment CTRL1 used the default CLM2.0 with the baseline runoff scheme.

[44] 2. Experiment CTRL2 was based on CTRL1; however, we implemented the subgrid precipitation scheme (equation (2)) to correct for overly large canopy interception of precipitation. Because GSWP2 data overcorrect snowfall, we used the monthly precipitation data of *Willmott and Matsuura* [2000] to constrain the three-hourly GSWP2 precipitation product in this experiment. The constrained precipitation mainly reduces snowfall in most cold regions.

[45] 3. On the basis of CTRL2, experiment SIMTOP-CB used a globally distributed $F_{\max}$ with the same formulation as experiment S2.

[46] 4. On the basis of CTRL2, experiment SIMTOP-EM used a globally distributed $F_{\max}$ with the same formulation as experiment S1. Through sensitivity experiments, we adjusted the parameters to f = 2.0 m^{-1} and $R_{sb,\max}$ = 1.0 × 10^{-4} mm s^{-1} and applied this adjustment globally in the experiments SIMTOP-CB and SIMTOP-EM. This study focuses on testing the framework of SIMTOP; therefore we do not address issues related to the scaling-up and optimization of these two calibration parameters.

Table 3. Results From Global Simulations Using the Baseline CLM 2.0 Runoff Model and SIMTOP[a]

	P	Total Runoff	R_{st}	RMSE	sm1	sm2	sm3
Observation	2.044*	0.801**	...	...	...	...	...
CTRL1	2.29	1.187	0.845	0.388	0.218	0.236	0.267
CTRL2	2.15	1.264	0.804	0.339	0.228	0.240	0.266
SIMTOP_CB	2.15	0.952	0.230	0.244	0.272	0.284	0.318
SIMTOP_EM	2.15	0.922	0.230	0.241	0.263	0.273	0.313

[a]This table shows the global land-averaged precipitation (P: mm/day), total runoff (mm/day), the ratio of surface runoff to total runoff (R_{st}), root mean square error (RMSE: mm/day) of runoff, and volumetric soil moisture of the top segment of the soil profile (sm1: 0.0–0.1 m), the middle segment of the soil profile (sm2: 0.1–1.0 m), and the lower segment of the soil profile (sm3: 1.0–3.43 m) for the four experiments on a global domain. * indicates that the estimated precipitation on land by *Peixoto and Oort* [1991]; ** indicates the UNH-GRDC runoff.

[47] CTRL1 exhibits unreasonably large canopy interception of precipitation, with particularly excessive interception loss in the Amazon River basin (Figure 10b). The subgrid precipitation scheme applied in experiment CTRL2 decreases the fractional area where the canopy can receive precipitation and thereby reduces the canopy water storage. Correspondingly, the interception loss is significantly decreased from 2.6 mm/day to 0.8 mm/day in rainy seasons (Figure 10b). Consequently, less precipitation is intercepted by the canopy in CTRL2 than in CTRL1; the increased amount of precipitation falling on the ground contributes more to increasing surface runoff (Figure 10c) than to increasing soil moisture (Figure 10d).

[48] The root mean square error of the simulated runoff is reduced from above 0.34 in CTRL1 and CTRL2 to below 0.244 in SIMTOP-EM and SIMTOP-CB (Table 3). In both CTRL1 and CTRL2, the peaks and troughs of runoff production occur about two months earlier than those of the UNH-GRDC runoff (Figure 10a). As both seasonal cycles are model derived, this difference may provide an estimate of the phase of the runoff production. However, since the fast-response surface runoff appears to be excessive relative to slow-response subsurface runoff (Figure 10c), the runoff we simulate in CTRL1 and CTRL2 is likely to occur too early. SIMTOP-EM and SIMTOP-CB produce much less surface runoff relative to subsurface runoff, when compared to CTRL1 and CTRL2. The ratio of surface runoff to total runoff, R_{st}, is 0.23 for both SIMTOP runs; for the control runs, R_{st} is above 0.8 (Table 3). Consequently, the timing of runoff production in SIMTOP-EM much better matches the timing of the UNH-GRDC runoff (Figure 10c). Less surface runoff also results in wetter soil (Figure 10d). We conclude that the partitioning of the total runoff and subsurface runoff is critical for the timing of runoff, the soil moisture content, and, hence, for the seasonality of evapotranspiration.

[49] SIMTOP-CB and SIMTOP-EM significantly improve the magnitude and timing of runoff simulation in tropical regions (Figures 11d–11f) and arid regions (Figures 11j–11l). However, the magnitude of the improvement in artic and boreal regions (Figures 11a–11c) and midlatitude regions (Figures 11g–11i) is not as great as in tropical and arid regions. This is because the current version of CLM neglects supercooled liquid water in frozen soil and the related treatment of hydraulic properties, which result in extremely low permeability and greater surface runoff (G.-Y. Niu and Z.-L. Yang, Parameterization of frozen soil and its impacts on snowmelt runoff and soil water storage, submitted to *Journal of Hydrometeorology*, 2005). In addition, the model produces shallower snow and earlier snowmelt than the observed in most midlatitude regions.

[50] SIMTOP-CB and SIMTOP-EM improve runoff simulation with almost the same volume of runoff (Figure 11), indicating that SIMTOP either with K_{sat} determined by the soil texture or with exponentially decaying K_{sat} and the surface macropores improves runoff simulation on global scales.

[51] The simulated runoff from SIMTOP-EM (0.95 mm/day) and SIMTOP-CB (0.92 mm/day) is about 0.15 mm/day (19%) and 0.12 mm/day (15%) greater than the UNH-DRDC runoff data, respectively (Table 3). This discrepancy is within the range of estimates from different global precipitation data sets, e.g. comparing global precipitation rate of the constrained GSWP2 data set (2.15 mm/day) with the estimate of 2.044 mm/day from *Peixoto and Oort* [1991]. In addition to the meteorological forcing data, there are many other model factors (e.g., vegetation parameters and soil hydraulic properties) that may affect the total amount of runoff. On the other hand, the UNH-GRDC runoff product may underestimate continental runoff because of its exclusion of river discharge from the catchments smaller than 25,000 km^2. Moreover, the hydrologic treatment described in CLM 2.0 neglected the presence of water reservoirs (rivers, lakes, wetlands, and man-made dams), which may explain a larger-than-observed magnitude of the annual mean discharge and a larger amplitude of the seasonal cycle of discharge [*Coe*, 2000]. *Vorosmarty et al.* [2004] reported that interception of river discharges by dams may reduce continental runoff by 20–25%.

6. Conclusions

[52] A simple TOPMODEL-based runoff scheme is developed for use in the NCAR CLM. SIMTOP simplifies TOPMODEL-based runoff scheme in two main ways. First, subsurface runoff in SIMTOP is a product of an exponential function of the water table depth and a single coefficient for maximum subsurface runoff. This coefficient is used in place of a complex product of four coefficients: α, $K_{sat}(0)$, $1/f$, and $e^{-\lambda_m}$, all of which are difficult to define on global scales.

[53] Use of a single maximum subsurface runoff coefficient also lessens the impact of the uncertainties inherent in computing the topographic index using coarse-resolution

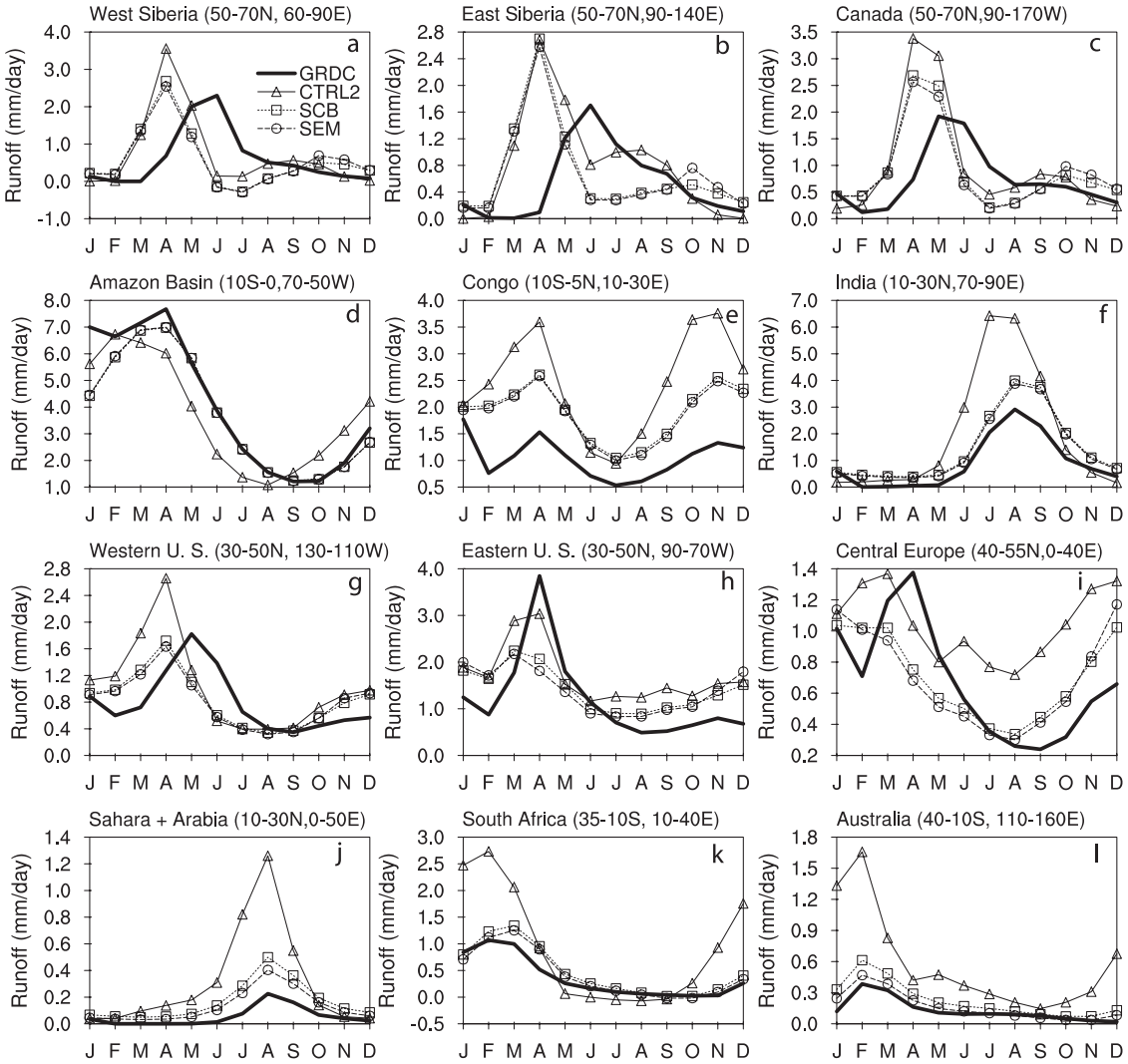

Figure 11. Modeled 10-year mean monthly runoff in comparison with the UNH-GRDC climatological monthly runoff in (a–c) arctic and boreal latitudes, (d–f) tropical latitudes, (g–i) midlatitudes, and (j–l) arid latitudes. ("SCB" in legend stands for SIMTOP-EM, which is called S1 in Table 2; "SEM" stands for SIMTOP-CB, which is called S2 in Table 2.)

DEM data. A constant value for the maximum subsurface runoff coefficient on the order of 10^{-4} mm s^{-1} works well when simulating runoff on a global scale. This change permits a TOPMODEL-based runoff scheme to work in SVATs without dramatically altering the value of K_{sat}, which is used by other model functions.

[54] Second, to parameterize the surface fractional saturated area, an exponential function is used to fit the discrete distribution of the topographic index. SIMTOP accommodates the topographic data using the maximum fractional saturated area, which is a parameter derived from the discrete distribution of the topographic index. The exponential function performs better than the commonly used three-parameter gamma distribution function in mountainous regions while preserving the accuracy in relatively flat regions.

[55] SIMTOP is validated against the runoff data for a small watershed and against global hydrologic data. SIMTOP has higher model efficiency than the baseline runoff model in CLM 2.0 both when K_{sat} decays exponentially with depth (with surface macropores) and when K_{sat} is defined by the soil texture profile data and a no-drainage boundary condition is imposed at the bottom of the soil column. The model partitioning of runoff into surface and subsurface components is very sensitive to $R_{sb,\max}$ and f that determines the hydrograph recession curve.

[56] **Acknowledgments.** This work was funded by NASA grant NAG5-10209, NAG5-12577 and NOAA grant NA03OAR4310076. The authors would like to acknowledge invaluable comments from Jay Famiglietti, Randy Koster, and two other anonymous reviewers. Marc Stieglitz is thanked for providing us with the Sleepers River watershed data set and the computer code to calculate the three-parameter gamma distribution function. Sarith Mahanama is thanked for providing us with IDL codes to process the HYDRO1K wetness index data. Texas Advanced Computing Center (TACC) is thanked for providing us with computing resources.

References

Beven, K. J. (1982), Macropores and water flow in soils, *Water Resour. Res.*, *18*, 1311–1325.

Beven, K. J. (1997), TOPMODEL: A critique, *Hydrol. Process.*, *11*(9), 1069–1085.

Beven, K. J., and M. J. Kirkby (1979), A physically based, variable contributing model of basin hydrology, *Hydrol. Sci. Bull.*, *24*, 43–69.

Bonan, G. B., K. W. Oleson, M. Vertenstein, S. Levis, X. Zeng, Y. Dai, R. E. Dickinson, and Z.-L. Yang (2002), The land surface climatology of the Community Land Model coupled to the NCAR Community Climate Model, *J. Clim.*, *15*, 3123–3149.

Boone, A., et al. (2004), The Rhone-aggregation land surface scheme intercomparison project: An overview, *J. Clim.*, *17*, 187–208.

Bowling, L. C., et al. (2003), Simulation of high latitude hydrological processes in the Torne-Kalix basin: PILPS Phase 2e. 1—Experimental description and summary intercomparisons, *Global Planet. Change*, *38*, 1–30.

Chen, J., and P. Kumar (2001), Topographic influence on the seasonal and inter-annual variation of water and energy balance of basins in North America, *J. Clim.*, *14*, 1989–2014.

Clapp, R. B., and G. M. Hornberger (1978), Empirical equations for some soil hydraulic properties, *Water Resour. Res.*, *14*, 601–604.

Coe, M. T. (2000), Modeling terrestrial hydrological systems at the continental scale: Testing the accuracy of an atmospheric GCM, *J. Clim.*, *13*, 686–704.

Cosby, B. J., G. M. Hornberger, R. B. Clapp, and T. R. Ginn (1984), A statistical exploration of the relationships of soil moisture characteristics to the physical properties of soils, *Water Resour. Res.*, *20*, 682–690.

Dai, Y., et al. (2003), The Common Land Model, *Bull. Am. Meteorol. Soc.*, *84*(8), 1013–1023.

Dickinson, R. E., A. Henderson-Sellers, and P. J. Kennedy (1993), Biosphere-Atmosphere Transfer Scheme (BATS) version 1e as coupled to the NCAR Community Climate Model, *NCAR Tech. Note*, *NCAR/TN-387+STR*, Natl. Cent. for Atmos. Res., Boulder, Colo.

Ducharne, A., R. D. Koster, M. J. Suarez, M. Stieglitz, and P. Kumar (2000), A catchment-based approach to modeling land surface processes in a general circulation model: 2. Parameter estimation and model demonstration, *J. Geophys. Res.*, *105*(D20), 24,823–24,838.

Entekhabi, D., and P. S. Eagleson (1989), Land surface hydrology parameterization for atmospheric general circulation models including subgrid-scale spatial variability, *J. Clim.*, *2*, 816–831.

Famiglietti, J. S., and E. F. Wood (1994), Multi-scale modeling of spatially variable water and energy balance processes, *Water Resour. Res.*, *30*(11), 3061–3078.

Fekete, B. M., C. J. Vorosmarty, and W. Grabs (2000), Global composite runoff fields based on observed discharge and simulated water balance, *Rep. 22*, Global Runoff Data Cent., Koblenz, Germany. (Available online at http://www.grdc.sr.unh.edu/html/paper/ReportUS.pdf)

Gedney, N., and P. M. Cox (2003), The sensitivity of global climate model simulations to the representation of soil moisture heterogeneity, *J. Hydrometeorol.*, *4*, 1265–1675.

Koster, R. D., M. J. Suarez, A. Ducharne, M. Stieglitz, and P. Kumar (2000), A catchment-based approach to modeling land surface processes in a general circulation model: 1. Model structure, *J. Geophys. Res.*, *105*(D20), 24,809–24,822.

Kumar, P. (2004), Layer averaged Richard's equation with lateral flow, *Adv. Water Resour.*, *27*(5), 522–532.

Liang, X., D. P. Lettenmaier, E. F. Wood, and S. J. Burges (1994), A simple hydrologically based model of land surface water and energy fluxes for general circulation models, *J. Geophys. Res.*, *99*, 14,415–14,428.

Niu, G.-Y., and Z.-L. Yang (2003), The Versatile Integrator of Surface and Atmosphere processes (VISA) Part II: Evaluation of three topography-based runoff schemes, *Global Planet. Change*, *38*, 191–208.

Oleson, K. W., et al. (2004), Technical description of the Community Land Model (CLM), *NCAR Tech. Note*, *NCAR/TN-461+STR*, Natl. Cent. for Atmos. Res., Boulder, Colo.

Peixoto, J. P., and A. H. Oort (1991), *Physics of Climate*, 520 pp., Am. Inst. of Phys., Melville, N. Y.

Quinn, P. F., J. Beven, and R. Lamb (1995), The $\ln(a/\tan\beta)$ index: How to calculate it and how to use it within the TOPMODEL framework, *Hydrol. Processes*, *9*, 161–182.

Sivapalan, M., K. Beven, and E. F. Wood (1987), On hydrologic similarity: 2. A scaled model of storm runoff production, *Water Resour. Res.*, *23*, 2266–2278.

Stieglitz, M., D. Rind, J. Famiglietti, and C. Rosenzweig (1997), An efficient approach to modeling the topographic control of surface hydrology for regional and global modeling, *J. Clim.*, *10*, 118–137.

Vorosmarty, C. J., et al. (2004), Humans transforming the global water system, *Eos Trans. AGU*, *85*(48), 509, 513–514.

Warrach, K., M. Stieglitz, H. T. Mengelkamp, and E. Raschke (2002), Advantages of a topographically controlled runoff simulation in a soil-vegetation-atmosphere transfer model, *J. Hydrometeorol.*, *3*, 131–148.

Willmott, C. J., and K. Matsuura (2000), Terrestrial air temperature and precipitation: Monthly and annual climatologies, Cent. for Clim. Res., Dep. of Geogr., Univ. of Del., Newark. (Available online at http://climate.geog.udel.edu/climate)

Wolock, D. M. (1993), Simulating the variable-source-area concept of watershed hydrology with TOPMODEL, *U.S. Geol. Surv. Water Resour. Invest. Rep. 93-4124*, 33 pp.

Wolock, D. M., and G. J. McCabe (1995), Comparison of single and multiple flow direction algorithms for computing topographic parameters in TOPMODEL, *Water Resour. Res.*, *31*, 1315–1324.

Wolock, D. M., and G. J. McCabe (2000), Differences in topographic characteristics computed from 100- and 1000-m resolution digital elevation model data, *Hydrol. Processes*, *14*, 987–1002.

Yang, Z.-L., and G.-Y. Niu (2003), The Versatile Integrator of Surface and Atmosphere Processes (VISA) part I: Model description, *Global Planet. Change*, *38*, 175–189.

Zhao, M., and P. A. Dirmeyer (2003), Production and analysis of GSWP-2 near-surface meteorology datasets, *COLA Tech. Rep. 159*, Cent. for Ocean-Land-Atmos. Stud., Calverton, Md. (Available online at http://grads.iges.org/gswp/)

R. E. Dickinson, School of Earth and Atmospheric Sciences, Georgia Institute of Technology, 311 Ferst Drive, Atlanta, GA 30332-0340, USA.

L. E. Gulden, G.-Y. Niu, and Z.-L. Yang, Department of Geological Sciences, John A. and Katherine G. Jackson School of Geosciences, University of Texas, Austin, TX 78712-0254, USA. (niu@geo.utexas.edu)